Cancer Science
Japanese Cancer Association JCA
Open Access

ZFP36L2 promotes cancer cell aggressiveness and is regulated by antitumor *microRNA-375* in pancreatic ductal adenocarcinoma

Keiichi Yonemori,[1] Naohiko Seki,[2] Hiroshi Kurahara,[1] Yusaku Osako,[1] Tetsuya Idichi,[1] Takayuki Arai,[2] Keiichi Koshizuka,[2] Yoshiaki Kita,[1] Kosei Maemura[1] and Shoji Natsugoe[1]

[1]Department of Digestive Surgery, Breast and Thyroid Surgery, Graduate School of Medical Sciences, Kagoshima University, Kagoshima; [2]Department of Functional Genomics, Chiba University Graduate School of Medicine, Chiba, Japan

Key words

MicroRNA, *miR-375*, pancreatic ductal adenocarcinoma, tumor-suppressor *ZFP36L2*

Correspondence

Hiroshi Kurahara, Department of Digestive Surgery, Breast and Thyroid Surgery, Graduate School of Medical Sciences Kagoshima University, Kagoshima 890-8520, Japan.
Tel: +81-99-275-5361; Fax: +81-99-265-7426;
E-mail: h-krhr@m3.kufm.kagoshima-u.ac.jp

Funding Information

No sources of funding were declared for this study.

Received July 21, 2016; Revised November 4, 2016; Accepted November 9, 2016

Cancer Sci **108** (2017) 124–135

doi: 10.1111/cas.13119

Due to its aggressive nature, pancreatic ductal adenocarcinoma (PDAC) is one of the most lethal and hard-to-treat malignancies. Recently developed targeted molecular strategies have contributed to remarkable improvements in the treatment of several cancers. However, such therapies have not been applied to PDAC. Therefore, new treatment options are needed for PDAC based on current genomic approaches. Expression of *microRNA-375* (*miR-375*) was significantly reduced in miRNA expression signatures of several types of cancers, including PDAC. The aim of the present study was to investigate the functional roles of *miR-375* in PDAC cells and to identify *miR-375*-regulated molecular networks involved in PDAC aggressiveness. The expression levels of *miR-375* were markedly downregulated in PDAC clinical specimens and cell lines (PANC-1 and SW1990). Ectopic expression of *miR-375* significantly suppressed cancer cell proliferation, migration and invasion. Our *in silico* and gene expression analyses and luciferase reporter assay showed that zinc finger protein 36 ring finger protein-like 2 (*ZFP36L2*) was a direct target of *miR-375* in PDAC cells. Silencing *ZFP36L2* inhibited cancer cell aggressiveness in PDAC cell lines, and overexpression of ZFP36L2 was confirmed in PDAC clinical specimens. Interestingly, Kaplan–Meier survival curves showed that high expression of ZFP36L2 predicted shorter survival in patients with PDAC. Moreover, we investigated the downstream molecular networks of the *miR-375*/*ZFP36L2* axis in PDAC cells. Elucidation of tumor-suppressive *miR-375*-mediated PDAC molecular networks may provide new insights into the potential mechanisms of PDAC pathogenesis.

Pancreatic ductal adenocarcinoma (PDAC) is one of the most lethal malignancies; despite recently developed treatments, the 5-year survival rate after diagnosis is only 5%.[1,2] PDAC cells are extremely aggressive and more than 50% of patients develop local recurrence or distant metastasis after curative resection.[1,3] PDAC frequently metastasizes to liver, peritoneum and lung.[4,5] Controlling recurrence and metastasis of PDAC improves disease prognosis. Therefore, understanding molecular mechanisms of PDAC aggressiveness through current genomic approaches is needed.

In the post-genome sequencing era, the discovery of non-coding RNA in the human genome provided new directions for the study of human cancer pathogenesis. MicroRNA (miRNA) belong to a family of small non-coding RNA and regulate expression of protein coding and non-coding RNA by repressing translation or cleaving RNA transcripts in a sequence-specific manner.[6] A unique characteristic of miRNA is that a single miRNA regulates a large number of RNA transcripts in human cells.[7] Thus, dysregulated miRNA expression disrupts tightly regulated RNA networks in cancer cells.[8] Currently, numerous studies have indicated that miRNA are aberrantly expressed in several cancers, including PDAC.[9,10] Using miRNA expression signatures, we have previously identified tumor-suppressive miRNA and the novel cancer networks controlled by these miRNA.[11–13]

We recently used the same method, miRNA expression signature, to identify aberrantly expressed miRNA in PDAC cells.[14] According to these miRNA signatures, *microRNA-375* (*miRNA-375*) was significantly reduced in cancer cells. The tumor-suppressive function of *miR-375* has been reported in several types of cancer.[15–18] Recent studies of PDAC cells showed that the anti-tumor function of *miR-375* is exerted by targeting several oncogenes, such as *PDK1* and *HOXB3*.[19,20] However, the RNA networks mediated by *miR-375* in PDAC are still obscure.

In this study, we focused on the functional significance of *miR-375* in PDAC cells by identifying the pathologic targets of *miR-375* and the RNA networks that contribute to PDAC aggressiveness. Our current study demonstrated that zinc finger protein 36 ring finger protein-like 2 (*ZFP36L2*) is directly regulated by tumor-suppressive *miR-375* in PDAC cells. ZFP36-family proteins bind to adenylate-uridylate (AU)-rich elements of mRNA, and control gene expression by degrading or inhibiting translation of the mRNA.[21,22] Interestingly, survival

analysis showed that high expression of ZFP36L2 predicted a significantly shorter survival of patients with PDAC. Elucidation of *miR-375*-mediated molecular networks in PDAC may provide new insights into the potential mechanisms of PDAC pathogenesis.

Materials and Methods

Clinical specimens and cell lines. Clinical tissue specimens ($n = 27$) and formalin-fixed, paraffin-embedded blocks ($n = 37$) were collected from patients with PDAC who underwent curative surgical resection at Kagoshima University Hospital between 1991 and 2014. Normal pancreatic tissue specimens ($n = 14$) were obtained from noncancerous tumor-adjacent tissue. Each surgical specimen was histologically classified according to the TNM classification system.[23] All patients in this study provided informed consent and the study protocol was approved by the Institutional Review Board of Kagoshima University. Two human PDAC cell lines were investigated in this study. PANC-1 cells were obtained from RIKEN Cell Bank (Tsukuba, Ibaraki, Japan) and SW 1990 cells were obtained from the ATCC (Manassas, VA, USA).

Total RNA, including miRNA, was isolated using ISOGEN (NIPPON GENE, Toyama, Japan) according to the manufacturer's protocol.

Quantitative RT-PCR. Quantification of miRNA was performed using quantitative RT-PCR (qRT-PCR) as previously described.[24–26] Briefly, miRNA were quantified using stem-loop RT-PCR, TaqMan MicroRNA Assays and Assay-on-Demand Gene Expression TaqMan probes and primers as directed by the manufacturer. Probes and primers for *miR-375* (product ID: 000564; Thermo Fisher Scientific, Kanagawa, Japan), *ZFP36L2* (product ID: Hs00272828_m1; Thermo Fisher Scientific), *CADM1* (product ID: Hs00942508_m1; Thermo Fisher Scientific), *TSPYL5* (product ID: Hs00603217_s1; Thermo Fisher Scientific), *ELFN2* (product ID: Hs00287464_s1; Thermo Fisher Scientific), *SLC7A5* (product ID: Hs01001183_m1; Thermo Fisher Scientific) and *HOMER1* (product ID: Hs01029333_m1; Thermo Fisher Scientific) were used. Human *GUSB* (product ID: Hs99999908_m1; Thermo Fisher Scientific) and *RNU48* (product ID: 001006; Thermo Fisher Scientific) were used as internal controls. Expression fold-changes were determined using the ΔΔCt method.

Transfection of miRNA mimic, inhibitor and siRNA into pancreatic ductal adenocarcinoma cell lines. Pancreatic ductal adenocarcinoma cell lines were transfected with a miRNA mimic for gain-of-function experiments, miRNA inhibitors for loss-of function experiments, and siRNA for loss-of-function experiments. Pre-miR miRNA precursors for *miR-375* (product ID: PM10327), negative control miRNA (product ID: AM 17111), two *ZFP36L2* siRNA (product IDs: HSS101105 and HSS101106) and negative control siRNA (product ID: D-001810-10) were purchased from Thermo Fisher Scientific. Two types of *miR-375* inhibitors (product ID: AM10327 and IH-300682-07-0005) were used: Thermo Fisher Scientific and GE Healthcare JAPAN (Tokyo, Japan). The transfection efficiencies of miRNA in PANC-1 and SW 1990 cells were calculated as described in previous studies.[24–26]

Cell proliferation, migration and invasion assays. Pancreatic ductal adenocarcinoma cells were transfected with 10 nmol/L miRNA or si-RNA by reverse transfection and seeded in 96-well plates at 5×10^3 cells per well. After 72 h, cell proliferation was evaluated by the XTT assay using a Cell Proliferation Kit II (Roche Molecular Biochemicals, Mannheim, Germany). Cell migration assays were performed with BD Falcon Cell Culture Inserts (BD Biosciences, Franklin Lakes, NJ, USA) that contained uncoated Transwell polycarbonate membrane filters with 8-μm pores in 24-well tissue culture plates. Cells were transfected with 10 nm miRNA or siRNA by reverse transfection and seeded in 6-cm dishes at 2×10^5 cells. After 48 h, the cells were collected and 1×10^5 cells were added to the upper chamber of each migration well and were allowed to migrate for 48 h. After gentle removal of the nonmigratory cells from the filter surface of the upper chamber, the cells that migrated to the lower side were fixed and stained with Diff-Quick (Sysmex Corporation, Kobe, Japan). The number of cells that migrated to the lower surface was determined microscopically by counting eight areas of constant size per well. Cell invasion assays were performed using modified Boyden chambers containing Transwell membrane filter inserts precoated with Matrigel with 8-μm pores in 24-well tissue culture plates (BD Biosciences, Bedford, MA, USA). All experiments were carried out in triplicate.

Western blot analyses. Protein lysates were collected 72 h after transfection and 20 μg of protein was separated using gel electrophoresis on e-PAGEL 5–20% gels (ATTO, Tokyo, Japan) before transfer to polyvinylidene fluoride membranes. Rabbit anti-ZFP36L2 antibodies (product ID: 2119; Cell Signaling Technology, Danvers, MA, USA) were diluted 1:1000 for immunoblotting. Anti-β actin antibodies at a 1:1000 dilution (product ID: A1978; Sigma Aldrich, St. Louis, MO, USA) were used as an internal loading control. A detailed description of the western blotting procedure is published elsewhere.[24–26]

Immunohistochemistry. Tissue sections were incubated overnight at room temperature with ZFP36L2 antibodies diluted 1:50 (product ID: HPA047428; Atlas Antibodies AB, Stockholm, Sweden). Following incubation, antibodies were visualized using an avidin–biotin complex (ABC) detection kit (Vector Laboratories, Burlingame, CA, USA) and a diaminobenzidine substrate system according to the manufacturer's protocol. Cytoplasmic staining of ZFP36L2 in at least 1% of cancer cells was classified as high. If no cancer cells were stained, specimens were classified as low for ZFP36L2 staining. The expression of ZFP36L2 was evaluated in 10 fields of 100 cells each using high-power microscopy (400 ×).

Genome-wide gene expression and *in silico* analyses. To identify *miR-375* target genes, a combination of genome-wide gene expression and *in silico* analyses was conducted as described previously.[24–26] The microarray data were deposited into the GEO repository under the accession numbers GSE77790 and GSE82108. Next, we selected putative miRNA target genes using the microRNA.org (August 2010 release, http://www.microrna.org/). Figure 1 shows the methodology for selecting target genes.

Plasmid construction and dual luciferase reporter assays. Partial wild-type sequences of the 3′-UTR of *ZFP36L2* containing the *miR-375* target site (positions 269–275 of *ZFP36L2* 3′-UTR, and positions 308-314 of *ZFP36L2* 3′-UTR for *miR-375*) or sequences with a deleted *miR-375* target site were inserted between the XhoI and PmeI restriction sites in the 3′-UTR of the hRluc gene in the psiCHECK-2 vector (product ID: C8021; Promega, Madison, WI, USA). PANC-1 and SW 1990 cell lines were transfected with 50 ng of the vector and 10 nM *miR-375* using Lipofectamine 2000 (Thermo Fisher Scientific) in Opti-MEM (Thermo Fisher Scientific). The activities of firefly and Renilla luciferases were determined in lysates of

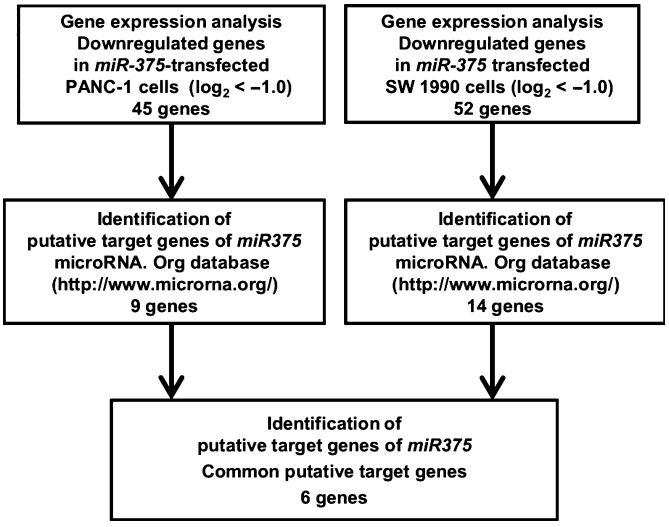

Fig. 1. Flow chart illustrating the analysis strategy for *miR-375* target genes. Expression analysis revealed 45 and 52 downregulated genes in *miR-375*-transfected PANC-1 and SW1990 pancreatic ductal adenocarcinoma (PDAC) cell lines, respectively. These were selected as putative target genes. Next, we compared the data of selected genes and the microRNA.org database. The analyses showed that 6 putative target genes were common to PANC-1 and SW 1990 *miR-375* transfectants. We then analyzed gene expression in available GEO datasets (accession number GSE82108).

transfected cells using a dual luciferase reporter assay system according to the manufacturer's recommendations (product ID: E1960; Promega, Madison, WI, USA). Data were normalized to firefly luciferase activity (ratio of Renilla/firefly luciferase activities).

Identification of downstream targets regulated by *ZFP36L2* in pancreatic ductal adenocarcinoma. We used genome-wide gene expression analysis in a PDAC cell line (PANC-1) transfected with si-ZFP36L2. Downregulated genes by *ZFP36L2* were categorized by KEGG pathways using the GENECODIS program pathways. Microarray results were deposited in the GEO database (accession number GSE82108).

Statistical analysis. Using expression values and the Mann–Whitney *U*-test or Bonferroni-adjusted Mann–Whitney *U*-test, relationships between two conditions or variables were analyzed. The correlation between expression of *miR-375* and *ZFP36L2* was evaluated using Spearman's rank test. Associations between different categories were assessed using Fisher's exact test and the χ^2-test. Overall survival (OS) after surgery was gauged using Kaplan–Meier curves. Patients were divided into two groups based on ZFP36L2 expression, and differences in survival were estimated using the log-rank test. Univariate and multivariate analyses were performed using the proportional hazards model. We used Expert StatView software (version 5.0 SAS Institute, Cary, NC, USA) for these analyses.

Results

Expression levels of *miR-375* in pancreatic ductal adenocarcinoma specimens and cell lines. We evaluated expression levels of *miR-375* in PDAC tissues ($n = 27$), normal pancreas tissues ($n = 14$) and two PDAC cell lines (PANC-1 and SW 1990). Patient backgrounds and clinicopathological characteristics are summarized in Table 1. The expression levels of *miR-375* were significantly lower in tumor tissues and PDAC cell lines compared with normal pancreas tissues (Fig. 2a). However, there were no significant relationships between any of the clinicopathological parameters (i.e. TNM stage, metastasis or survival rate) and the expression of *miR-375* (Fig. S1).

Effect of *miR-375* expression on cell growth, migration and invasion in pancreatic ductal adenocarcinoma cell lines. To investigate the functional roles of *miR-375*, we performed gain-of-function studies using transfection. XTT, cell migration and cell invasion assays demonstrated that cell proliferation, migration and invasion were significantly inhibited in *miR-375* transfectants compared with mock or miR-control transfectants (each $P < 0.0001$, Fig. 2b–d). Furthermore, we performed loss-of-function assays using *miR-375* inhibitors in PDAC cells. Our present data showed that cancer cell proliferation, migration and invasion were significantly enhanced by suppression of *miR-375* in PDAC cells (Fig. S2). These results suggested that *miR-375* could have a tumor-suppressive function in PDAC cells.

Identification of genes regulated by *miR-375* in pancreatic ductal adenocarcinoma cells. To gain further insight into the molecular mechanisms and pathways regulated by tumor-suppressive *miR-375* in PDAC cells, we used a combination of *in silico* and gene expression analyses. Figure 1 presents the strategy for narrowing down the target genes of *miR-375*. In gene expression analyses, 45 and 52 genes were downregulated ($\log_2$ ratio <-1.0) in PANC-1 and SW 1990 *miR-375* transfectants, respectively, in comparison with control transfectants (GEO accession number GSE77790). Next, we pared down the list of genes using the microRNA.org database. We found that 9 and 14 genes were putatively targeted by *miR-375* in PANC-1 and SW 1990 *miR-375* transfectants, respectively. Of those genes, 6 were common to both *miR-375* transfectants. We validated the changes of 6 genes by *miR-375* regulation using *miR-375* transfectant cells (Fig. S3). Among them, we determined that *ZFP36L2* was upregulated in clinical PDAC samples using qRT-PCR (Table 3, Fig. 3a,c). No negative correlations between *miR-375* expression and *ZFP36L2* mRNA expression were found using Spearman's rank test ($r = -0.240$, $P = 0.1042$, Fig. 3b).

***ZFP36L2* is a direct target of *miR-375* in pancreatic ductal adenocarcinoma cells.** We performed qRT-PCR to validate *miR-375* repression of *ZFP36L2* mRNA expression in PDAC cell lines. Our studies revealed that *ZFP36L2* mRNA was significantly reduced in *miR-375* transfectants in comparison with mock or miR-control transfectants ($P < 0.0001$ and $P = 0.0036$, Fig. 4a). Protein expression of *ZFP36L2* was also repressed in the *miR-375* transfectants (Fig. 4b).

Target prediction databases indicated two putative target sites in the 3′-UTR of *ZFP36L2* (Fig. 4c). To determine whether *ZFP36L2* mRNA had a functional target site, we performed a luciferase reporter assay. Compared with the miR-control, luminescence intensity was significantly reduced by transfection with *miR-375* at the *miR-375* target site, position 308-314 in the 3′-UTR of *ZFP36L2* (Fig. 4c, lower).

Effects of silencing *ZFP36L2* on PDAC cell lines. To investigate the functional role of *ZFP36L2* in PDAC cells, we carried out loss-of-function studies using si-*ZFP36L2* transfectants. First, we evaluated the knockdown efficiency of si-*ZFP36L2* transfection in PDAC cell lines. In the present study, we used two types of si-*ZFP36L2* (si-*ZFP36L2-1* and si-*ZFP36L2-2*). According to qRT-PCR and western blot analyses, both siRNA effectively downregulated *ZFP36L2* expression in both cell lines (Fig. 5a,b). XTT, cell migration and cell invasion assays demonstrated that cell proliferation, migration and invasion

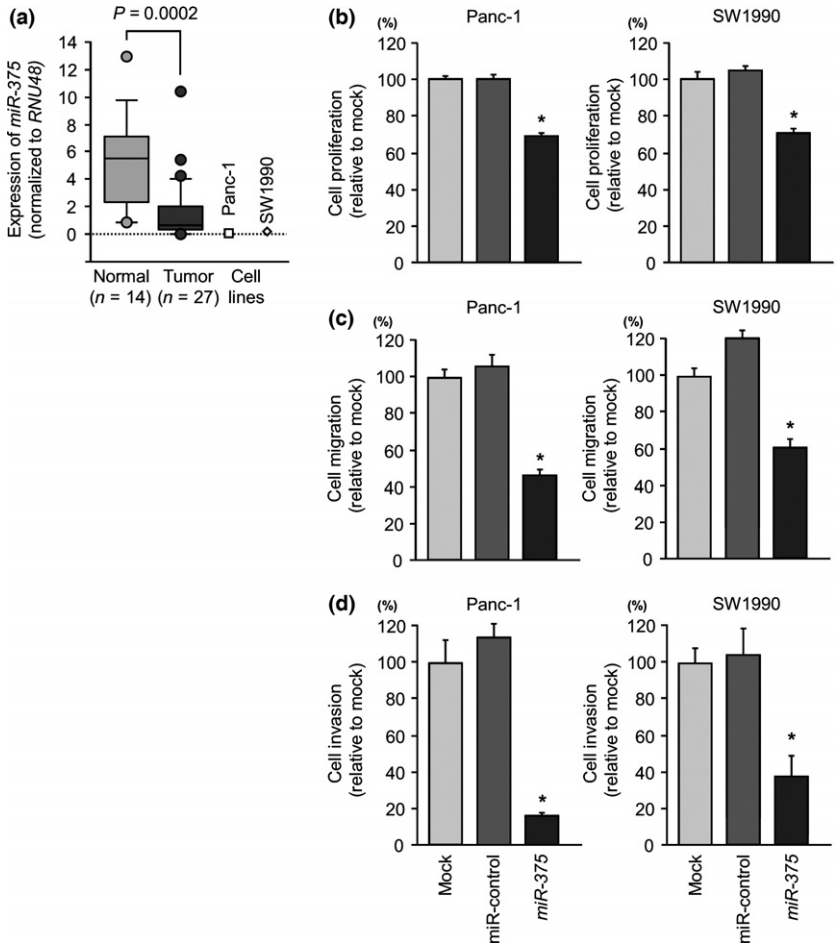

Fig. 2. Expression levels of *miR-375* and its effects on pancreatic ductal adenocarcinoma (PDAC) cells. (a) Expression levels of *miR-375* in clinical specimens and PDAC cell lines were determined using quantitative RT-PCR (qRT-PCR). Data were normalized to *RNU48* expression. (b) Cell growth was determined using XTT assay 72 h after transfection with 10 nM *miR-375*. $*P < 0.0001$. (c) Cell migration activity was determined using BD Falcon Cell Culture Inserts. $*P < 0.0001$. (d) Cell invasion activity was determined using Matrigel invasion assays. $*P < 0.0001$.

Table 1. Characteristics of the patients

Pancreatic ductal adenocarcinoma	
Total number	27
Median age (range), years	67.1 (42–85)
Gender	
Male	12
Female	15
T category	
pTis	1
pT1	2
pT2	0
pT3	22
pT4	2
N category	
0	14
1	13
M category	
0	25
1	2
Neoadjuvant chemotherapy	
(−)	12
(+)	15
Recurrence	
(−)	11
(+)	16
Normal pancreas tissue	
Total number	14

Table 2. Characteristics of patients included in the immunohistochemistry

Pancreatic ductal adenocarcinoma	
Total number	37
Median age (range), years	66.9 (44–85)
Gender	
Male	21
Female	16
T category	
pTis	0
pT1	0
pT2	2
pT3	26
pT4	9
N category	
0	14
1	23
M category	
0	37
1	0
Neoadjuvant chemotherapy	
(−)	37
(+)	0
Recurrence	
(−)	8
(+)	29

Table 3. Candidate target genes regulated by *miR-375* in pancreatic ductal adenocarcinoma

Entrez gene ID	Gene symbol	Description	Microarray (Log_2 ratio) *miR-375*			Target site (miRanda)
			Panc-1	SW1990	Average	*miR-375*
23705	*CADM1*	Cell adhesion molecule 1	−3.86	−5.17	−4.51	(+)
9456	*HOMER1*	Homer scaffolding protein 1	−1.76	−1.77	−1.76	(+)
8140	*SLC7A5*	Solute carrier family 7 member 5	−1.51	−1.52	−1.52	(+)
85453	*TSPYL5*	TSPY-like 5	−1.38	−1.38	−1.38	(+)
678	*ZFP36L2*	ZFP36 ring finger protein-like 2	−1.20	−1.04	−1.12	(+)
114794	*ELFN2*	Extracellular leucine-rich repeat and fibronectin type III domain containing 2	−1.00	−1.13	−1.07	(+)

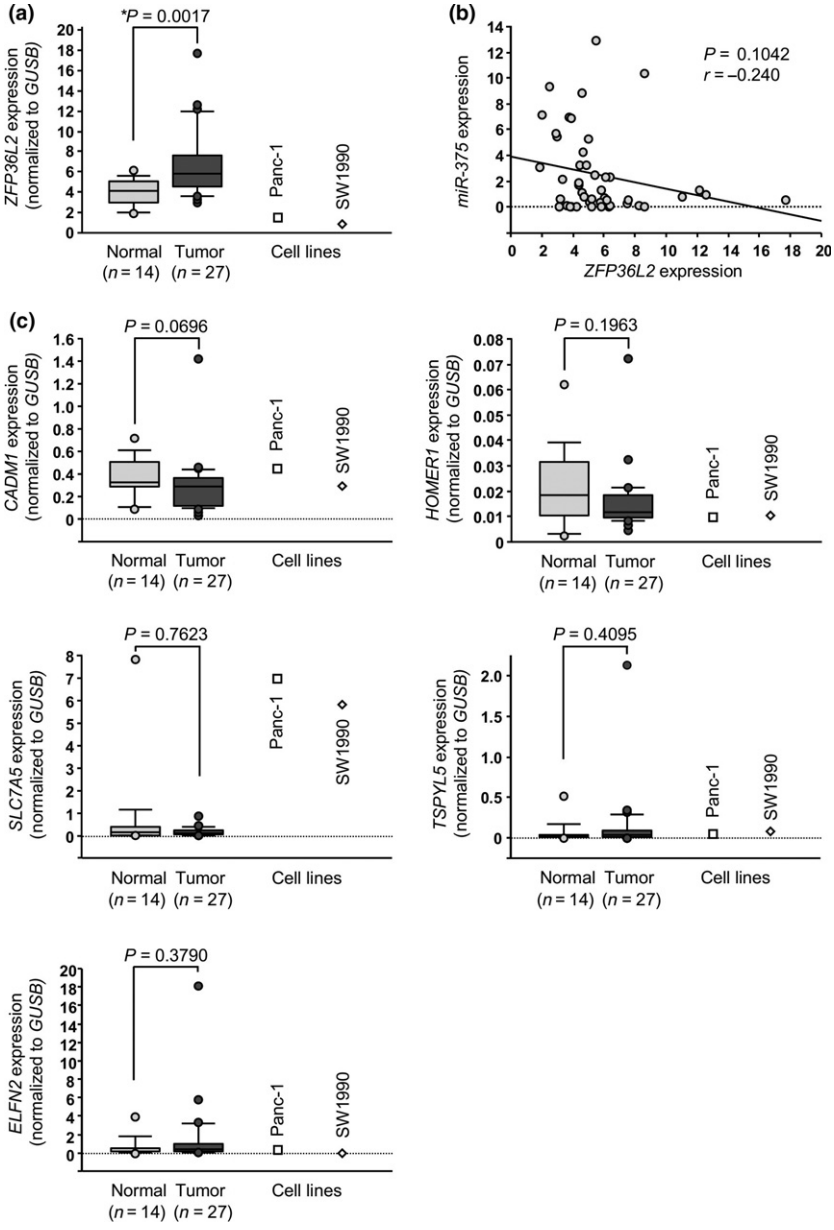

Fig. 3. Expression of putative *miR-375* target genes in pancreatic ductal adenocarcinoma (PDAC) clinical specimens and cell lines. (a) Expression levels of *ZFP36L2* in clinical specimens and PDAC cell lines were determined using quantitative RT-PCR (qRT-PCR). Data were normalized to *GUSB* expression. (b) Correlation between *miR-375* and *ZFP36L2* expression. (c) Expression levels of other putative *miR375* target genes in clinical specimens and PDAC cell lines were determined using qRT-PCR. Data were normalized to *GUSB* expression.

were inhibited in si-*ZFP36L2* transfectants compared with mock-control or siRNA-control-transfected cells (Fig. 5c–e).

Expression of ZFP36L2 in pancreatic ductal adenocarcinoma clinical specimens. We confirmed the expression of ZFP36L2 in PDAC clinical specimens using immunohistochemistry. A total of 37 specimens were evaluated, and 13 samples were classified as having high expression of ZFP36L2 (Fig. 6a–c). Clinicopathological characteristics are summarized in Table 2.

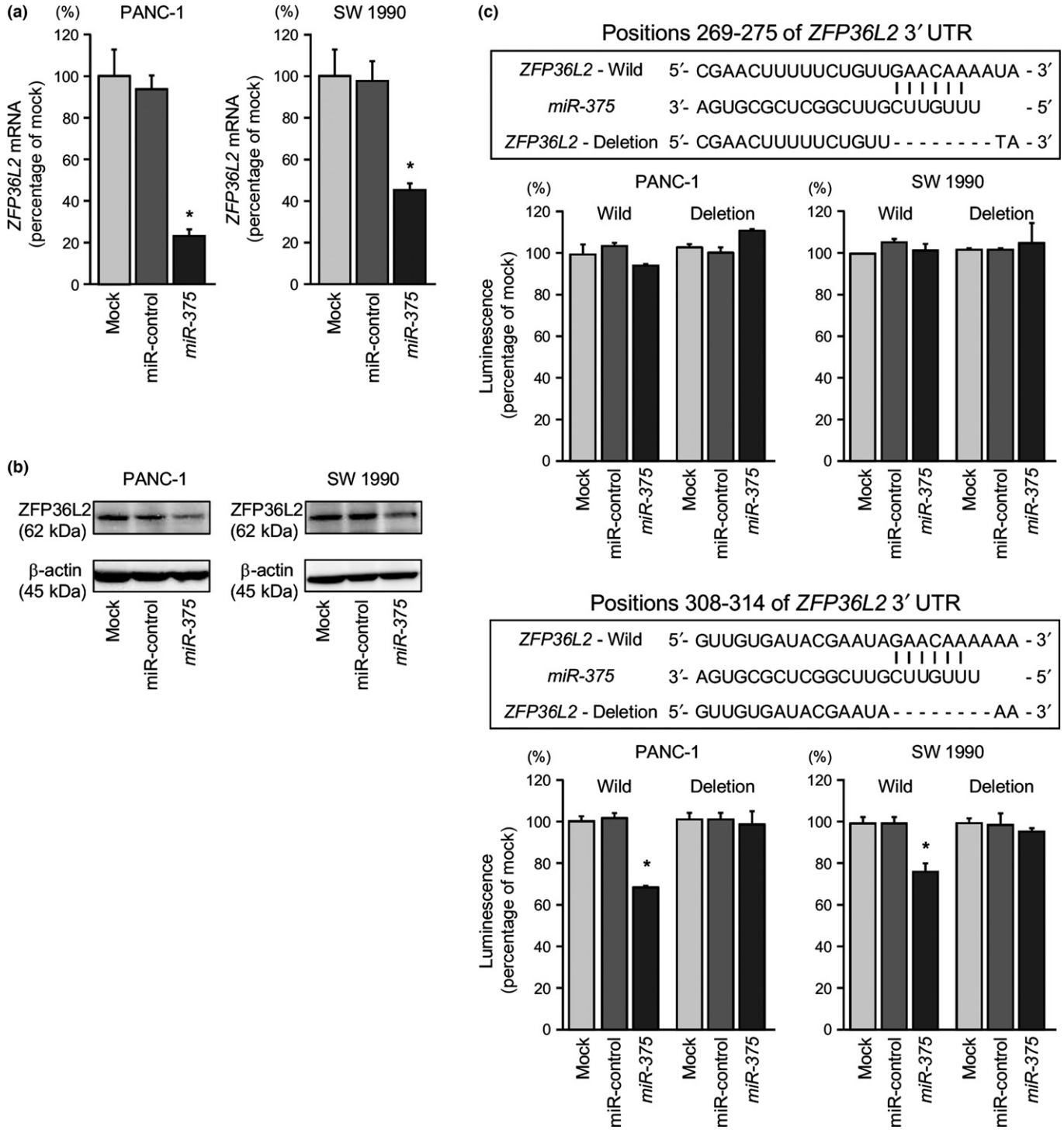

Fig. 4. Direct regulation of *ZFP36L2* by *miR-375* in pancreatic ductal adenocarcinoma (PDAC) cells. (a) *ZFP36L2* mRNA expression was evaluated using quantitative RT-PCR (qRT-PCR) in PANC-1 and SW1990 cells 72 h after transfection with *miR-375*. *GUSB* was used as an internal control. **P* < 0.0001. (b) ZFP36L2 protein expression was evaluated using western blot in PANC-1 and SW1990 cells 72–96 h after transfection with *miR-375*. β-actin was used as a loading control. (c) *miR-375* binding sites in the 3′-UTR of *ZFP36L2* mRNA. Dual luciferase reporter assays using vectors encoding putative *miR-375* target sites of the *ZFP36L2* 3′-UTR (positions 269–275 and 308–314) for both wild-type and deleted regions. Data were normalized as ratios of *Renilla*/firefly luciferase activities. **P* < 0.0001.

Table 4 shows the correlation between ZFP3L2 expression and various clinicopathological factors. High ZFP36L2 expression was significantly associated with increased lymph node metastasis. Furthermore, patients with high ZFP36L2 expression had significantly shorter OS than those with low ZFP36L2 expression ($P = 0.0167$) (Fig. 6d). In addition, univariate and multivariate analysis showed that ZFP36L2 served as an independent prognostic factor for PDAC (Table 5).

Investigation of downstream genes regulated by *ZFP36L2* in pancreatic ductal adenocarcinoma cells. To identify the

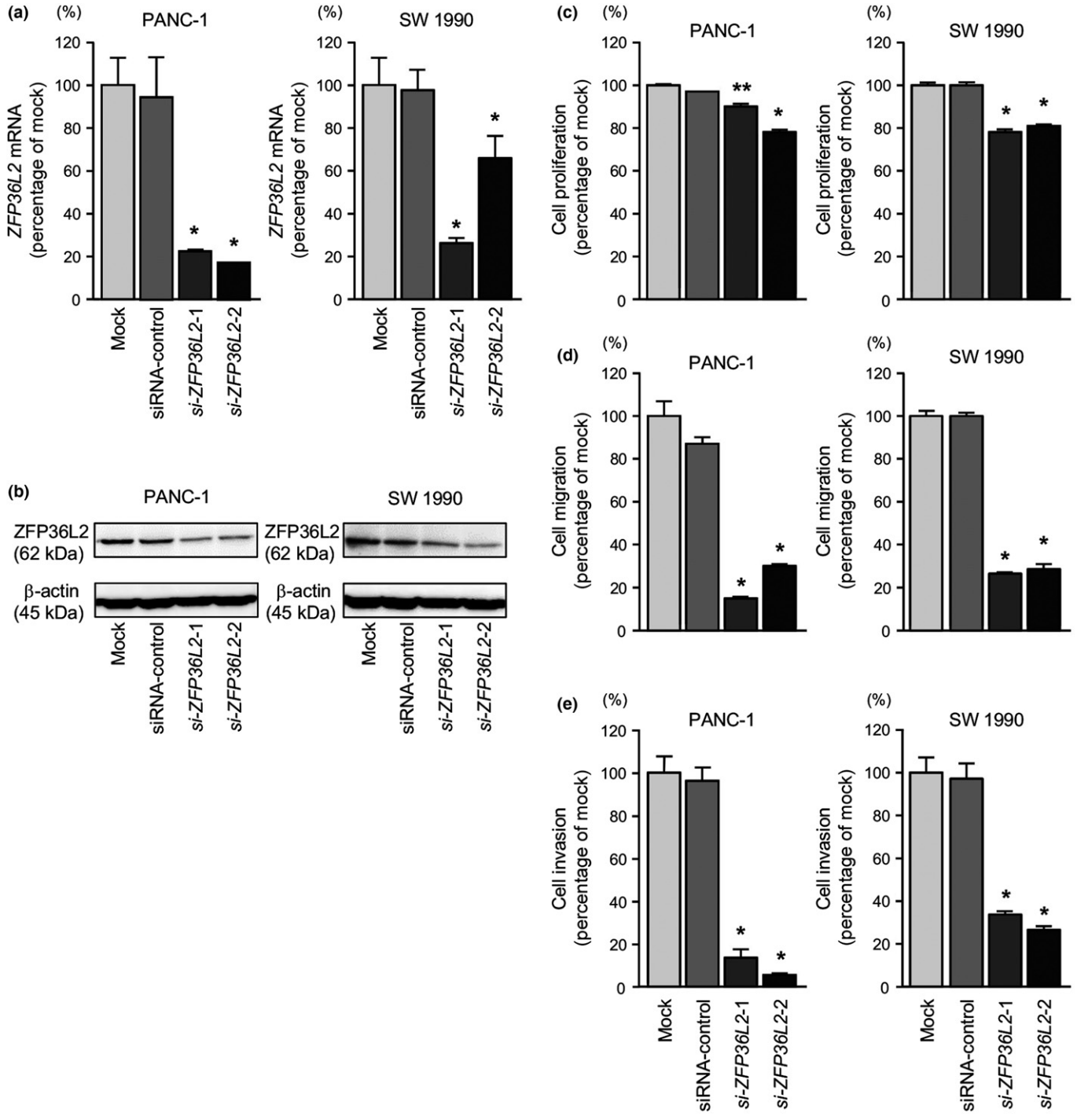

Fig. 5. Effects of *ZFP36L2* silencing on pancreatic ductal adenocarcinoma (PDAC) cell lines. (a) *ZFP36L2* mRNA expression was evaluated using quantitative RT-PCR (qRT-PCR) in PANC-1 and SW1990 cells 72 h after transfection with *si-ZFP36L2*-1 and *si-ZFP36L2*-2. *GUSB* was used as an internal control. (b) ZFP36L2 protein expression was evaluated using western blot in PANC-1 and SW1990 cells 72 to 96 h after transfection with *miR-375*. β-actin was used as a loading control. (c) Cell proliferation was determined using XTT assay 72 h after transfection with 10 nM *si-ZFP36L2*-1 or *si-ZFP36L2*-2. $*P < 0.0001$, $**P = 0.0007$. (d) Cell migration activity was determined using BD Falcon Cell Culture Inserts. $*P < 0.0001$. (e) Cell invasion activity was determined using Matrigel invasion assays. $*P < 0.0001$.

downstream genes regulated by *ZFP36L2*, genome-wide gene expression and *in silico* analyses were performed in a PDAC cell line (PANC-1) transfected with si-*ZFP36L2*. A total of 1287 genes were commonly downregulated ($\log_2$ ratio < -1.0) in si-*ZFP36L2*-transfected PANC-1 cells. We also assigned the downregulated genes to KEGG pathways using the GENECODIS program and identified 60 pathways as significantly enriched. The 5 most enriched pathways are presented in Table 6a. Of these 5 pathways, we focused on genes in the 'cell cycle' and 'pathways in cancer' pathways. The genes composing these 2 pathways are listed in Table 6b,c. Furthermore, we checked the expression status of these genes and

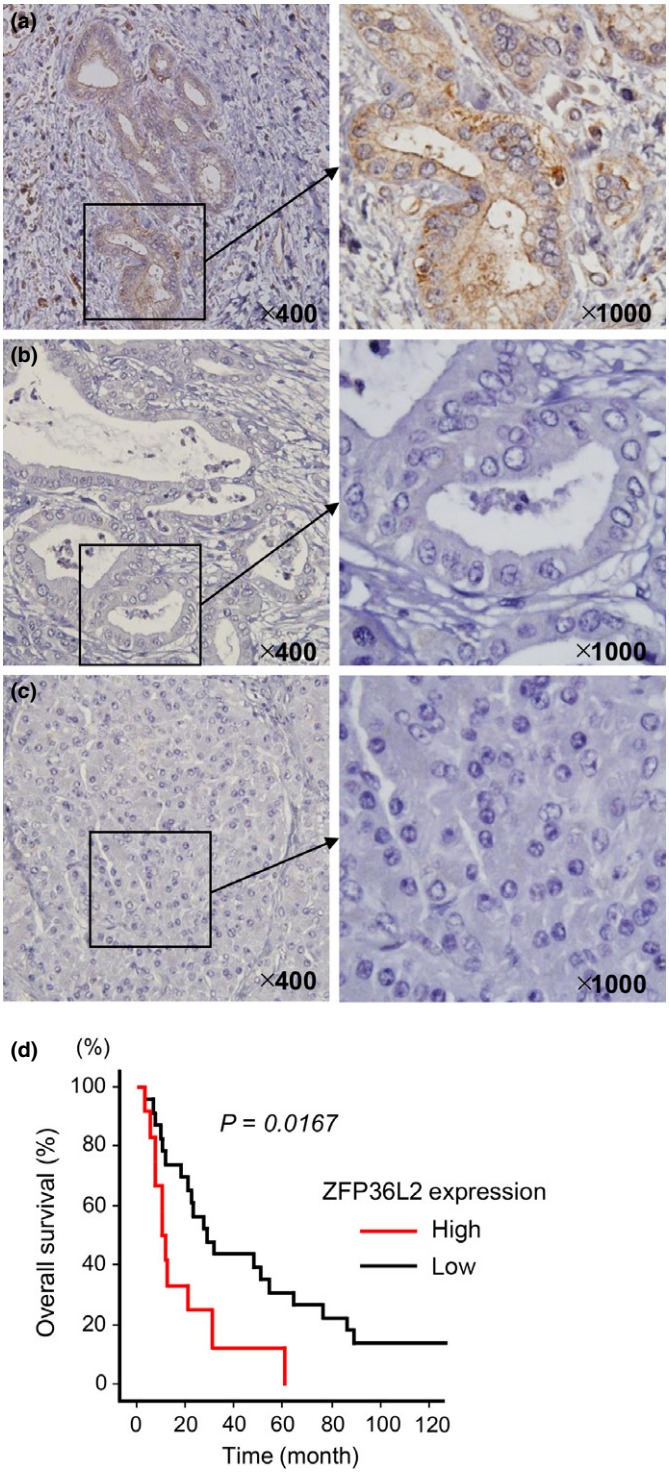

Fig. 6. Immunohistochemical staining of ZFP36L2 in pancreatic ductal adenocarcinoma (PDAC) clinical specimens and association of ZFP36L2 with overall survival. Immunohistochemical staining of ZFP36L2 in PDAC clinical specimens. Overexpression of ZFP36L2 was observed in cancer lesions (original magnification ×400). In contrast, negative staining of ZFP36L2 was observed in normal tissues. (a) Positively stained cancer lesion (T3N1M0). (b) Negatively stained cancer lesion (T3N1M0). (c) Negatively stained normal pancreas tissue. (d) Kaplan–Meier survival curves for overall survival rates based on ZFP36L2 expression in 37 patients with PDAC. *P*-values were calculated using the log-rank test.

Table 4. Correlation between the expression of *ZFP36L2* and clinicopathological factors in pancreatic ductal adenocarcinoma (*n* = 37)

Characteristic	*ZFP36L2*		*P*
	Low (*n* = 24)	High (*n* = 13)	
Age (*n*)			
≥60 (26)	15	11	NS
<60 (11)	9	2	
Gender (*n*)			
Male (21)	13	8	
Female (16)	11	5	NS
Tumor size (*n*)			
>40 mm (9)	4	5	NS
≤40 mm (28)	20	8	
Lymph node metastasis (*n*)			
No (14)	12	2	0.0382
Yes (23)	12	11	
TNM Stage (*n*)			
I/II (27)	17	10	NS
III/IV (10)	7	3	
Recurrence (*n*)			
No (8)	7	1	NS
Yes (29)	17	12	

Table 5. Univariate analysis and multivariate analysis in pancreatic ductal adenocarcinoma

Univariate analysis	Hazard ratio	95% CI	*P*-value
Age	0.971	0.490–1.926	0.9333
Gender	0.405	0.206–0.795	0.0086
Tumor size	1.544	0.737–3.236	0.2499
Lymph node metastasis	0.584	0.294–1.161	0.1248
Distant metastasis	0.436	0.176–1.076	0.0716
TNM stage	2.321	1.174–4.587	0.0154
ZFP36L2	0.383	0.186–0.788	0.0091
Multivariate analysis			
Gender	0.302	0.147–0.620	0.0011
TNM stage	3.792	1.777–8.091	0.0006
ZFP36L2	0.269	0.123–0.585	0.0009

pathologic relations of the PDAC by using TCGA-based large cohort study data (Table 6b,c). We applied the OncoLnc database using 87 pancreatic adenocarcinoma samples (http://www.oncolnc.org/). Clinical outcome for patients with high expression of *CCNB1* and *CCNB2* or low expression of these genes are displayed as Kaplan–Meier plots with log-rank tests (Fig. S4).[27]

Discussion

Most patients with PDAC already have advanced or metastasized cancer at the time of first diagnosis. The prognosis for patients with advanced stage PDAC is extremely poor, and there are few effective treatments to date.[28] An oncogenic *KRAS* mutation is frequently observed in patients with PDAC and leads to constitutive activation of *KRAS* downstream signaling pathways.[29] Many studies have failed to directly

Table 6. (a) Top 5 enriched KEGG pathways downregulated by si-*ZFP36L2*; (b) Regulation of genes related to the cell cycle; (c) Regulation of genes related to the pathways in cancer

(a) Number of genes	Pathway name	*P*-value
26	Cell cycle	2.25E-16
20	Oocyte meiosis	1.23E-11
30	Pathways in cancer	4.32E-09
14	Small cell lung cancer	4.67E-08
14	Progesterone-mediated oocyte maturation	6.36E-08

(b) Cell cycle

Entrez gene ID	Gene symbol	Gene name	PANC-1 $\log_2$ ratio	GEO data (GSE 15471)	OncoLnc *P*-value
8318	*CDC45*	Cell division cycle 45	−2.02	2.97	0.00269
8243	*SMC1A*	Structural maintenance of chromosomes 1A	−1.59	11.23	NS
7029	*TFDP2*	Transcription factor Dp-2 (E2F dimerization partner 2)	−1.57	No data	0.00226
5933	*RBL1*	Retinoblastoma-like 1	−1.49	No data	NS
5347	*PLK1*	Polo-like kinase 1	−1.38	No data	0.00729
1021	*CDK6*	Cyclin-dependent kinase 6	−1.36	2.67	<0.001
4087	*SMAD2*	SMAD family member 2	−1.36	No data	NS
10744	*PTTG2*	Pituitary tumor-transforming 2	−1.35	No data	No data
9133	*CCNB2*	Cyclin B2	−1.35	6.78	<0.001
25847	*ANAPC13*	Anaphase promoting complex subunit 13	−1.28	No data	NS
7042	*TGFB2*	Transforming growth factor, beta 2	−1.25	2.62	NS
996	*CDC27*	Cell division cycle 27	−1.21	2.96	NS
4193	*MDM2*	MDM2 proto-oncogene, E3 ubiquitin protein ligase	−1.20	2.35	NS
9700	*ESPL1*	Extra spindle pole bodies homolog 1 (*S. cerevisiae*)	−1.19	No data	NS
1869	*E2F1*	E2F transcription factor 1	−1.17	No data	0.00152
9232	*PTTG1*	Pituitary tumor-transforming 1	−1.15	No data	NS
983	*CDK1*	Cyclin-dependent kinase 1	−1.14	2.11	0.00137
10735	*STAG2*	Stromal antigen 2	−1.13	No data	NS
699	*BUB1*	BUB1 mitotic checkpoint serine/threonine kinase	−1.13	2.61	0.00515
891	*CCNB1*	Cyclin B1	−1.11	4.77	0.00710
4174	*MCM5*	Minichromosome maintenance complex component 5	−1.10	No data	NS
995	*CDC25C*	Cell division cycle 25C	−1.08	No data	0.00457
51434	*ANAPC7*	Anaphase promoting complex subunit 7	−1.06	No data	NS
6502	*SKP2*	S-phase kinase-associated protein 2, E3 ubiquitin Protein ligase	−1.05	No data	NS
10971	*YWHAQ*	Tyrosine 3-monooxygenase/tryptophan 5-monooxygenase activation protein, theta	−1.04	2.51	NS
10274	*STAG1*	Stromal antigen 1	−1.01	No data	NS

(c) Pathways in cancer

Entrez gene ID	Gene symbol	Gene name	PANC-1 $\log_2$ ratio	GEO data (GSE 15471)	OncoLnc *P*-value
4312	*MMP1*	Matrix metallopeptidase 1 (interstitial collagenase)	−3.08	11.23	NS
6513	*SLC2A1*	Solute carrier family 2 (facilitated glucose transporter), member 1	−2.26	2.67	0.02410
1956	*EGFR*	Epidermal growth factor receptor	−2.06	No data	0.00674
7422	*VEGFA*	Vascular endothelial growth factor A	−1.97	No data	NS
5290	*PIK3CA*	Phosphatidylinositol-4,5-bisphosphate 3-kinase, catalytic subunit alpha	−1.82	No data	NS
1499	*CTNNB1*	Catenin (cadherin-associated protein), beta 1, 88 kDa	−1.66	2.35	NS
3918	*LAMC2*	Laminin, gamma 2	−1.65	6.78	NS
3655	*ITGA6*	Integrin, alpha 6	−1.56	No data	0.0388
3675	*ITGA3*	Integrin, alpha 3 (antigen CD49C, alpha 3 subunit of VLA-3 receptor)	−1.42	2.51	<0.001
5291	*PIK3CB*	Phosphatidylinositol-4,5-bisphosphate 3-kinase, catalytic subunit beta	−1.40	No data	0.00681
207	*AKT1*	v-akt murine thymoma viral oncogene homolog 1	−1.40	No data	NS
3910	*LAMA4*	Laminin, alpha 4	−1.37	4.77	NS
1021	*CDK6*	Cyclin-dependent kinase 6	−1.36	No data	<0.001
4087	*SMAD2*	SMAD family member 2	−1.36	No data	NS
6772	*STAT1*	Signal transducer and activator of transcription 1	−1.33	2.96	0.01520
8453	*CUL2*	Cullin 2	−1.29	No data	NS

Table 6 (Continued)

(c) Pathways in cancer

Entrez gene ID	Gene symbol	Gene name	PANC-1 log_2 ratio	GEO data (GSE 15471)	OncoLnc *P*-value
7042	*TGFB2*	Transforming growth factor, beta 2	−1.25	2.62	NS
5899	*RALB*	v-ral simian leukemia viral oncogene homolog B	−1.24	No data	<0.001
4193	*MDM2*	MDM2 proto-oncogene, E3 ubiquitin protein ligase	−1.20	No data	NS
7477	*WNT7B*	Wingless-type MMTV integration site family, member 7B	−1.19	No data	NS
208	*AKT2*	v-akt murine thymoma viral oncogene homolog 2	−1.18	No data	NS
1869	*E2F1*	E2F transcription factor 1	−1.17	No data	0.00152
355	*FAS*	Fas cell surface death receptor	−1.13	2.97	0.03640
330	*BIRC3*	Baculoviral IAP repeat containing 3	−1.13	2.61	NS
4824	*NKX3-1*	NK3 homeobox 1	−1.11	No data	NS
3091	*HIF1A*	Hypoxia inducible factor 1, alpha subunit (basic helix-loop-helix transcription factor)	−1.10	2.11	NS
6502	*SKP2*	S-phase kinase-associated protein 2, E3 ubiquitin protein ligase	−1.05	No data	NS
5728	*PTEN*	Phosphatase and tensin homolog	−1.05	No data	NS
2250	*FGF5*	Fibroblast growth factor 5	−1.02	No data	0.04710
7186	*TRAF2*	TNF receptor-associated factor 2	−1.01	No data	NS

NS, not significant. OncoLnc, OncoLnc database.

inhibit activation of KRAS, suggesting that *KRAS* is a non-druggable target in human cancers.[29] To develop new treatment strategies for the disease, it is necessary to elucidate the molecular pathogenesis of PDAC aggressiveness using current genomic approaches.

Substantial evidence has demonstrated that aberrant expression of miRNA is deeply involved in human cancer pathogenesis, including that of PDAC.[14,30] Functionally, miRNA fine-tune expression of protein-coding and non-coding RNA in human cells.[31] Therefore, aberrantly expressed miRNA lead to the collapse of tightly regulated RNA networks in cancer cells. Recently, we summarized the aberrant expression of miRNA in PDAC cells.[14] Several miRNA were significantly downregulated in PDAC cells, such as *miR-217*, *miR-141*, *miR-148a*, *miR-375* and *miR-29c*. Recent studies have also demonstrated that these miRNA function as antitumor miRNA in PDAC.[32–34] For example, expression of *miR-217* was significantly reduced in PDAC tissues and cell lines and directly targeted *KRAS* mRNA.[32] It is well known that *miR-200c/miR-141* form a miRNA cluster and inhibit epithelial–mesenchymal transition (EMT) in cancer cells.[35,36] In PDAC, *miR-200c* and *miR-141* directly bind to the 3′-UTR of *ZEB1* mRNA and *TGFb* mRNA, respectively, and inhibit cell invasion and migration.[33] *MiR-148a* has been reported to be associated with DNA methylation in malignant tumors, including PDAC.[34]

Our previous studies showed that expression of *miR-375* was markedly reduced in several types of cancers and functions as an antitumor miRNA.[37–39] Other studies confirm the antitumor function of *miR-375* in cancer.[40,41] In contrast to these antitumor activities, expression of *miR-375* was upregulated in pediatric acute myeloid leukemia and prostate cancer, suggesting that *miR-375* acts as an oncogenic miRNA in these diseases.[42,43] The dual function of *miR-375* is very unique; thus, it is important to identify *miR-375*-regulated pathways in various cancer types. In this study, we focused on *miR-375* and *miR-375*-mediated oncogenic pathways in PDAC. Previous studies of *miR-375* in PDAC indicated that pyruvate dehydrogenase kinase, isozyme 1 (*PDK1*) is a regulatory target of *miR-375*. PDK1 is a key component in the phosphatidylinositol 3-kinase-Akt-mammalian target of rapamycin (PI3K-Akt-mTOR) signaling pathway and has been shown to inhibit proliferation and promote apoptosis in PDAC cells.[19,44]

In this study, we showed that ectopic expression of *miR-375* significantly suppressed cancer cell aggressiveness and confirmed the antitumor function of *miR-375* in PDAC cells. Moreover, we identified that *ZFP36L2* was directly regulated by antitumor *miR-375* in PDAC cells. *ZFP36L2* is zinc finger protein 36, C3H type-like 2 (also known as *Brf2*, *Erf2* and T*is11D*).[22] *ZFP36L2* directly binds to the AU-rich element (ARE) in the 3′-UTR of the target mRNA and regulates the expression of target mRNA.[21,22]

According to the previous studies, *ZFP36* has antitumor function in several types of cancers.[22,45] Past studies have shown that deletion of *ZFP36L2* induced Notch1-dependent T cell acute lymphoblastic leukemia in mice, and a frameshift mutation in the *ZFP36L2* gene was identified in several types of leukemic cells.[46] In leukemic cells, a heterozygous frameshift mutation of ZFP36L2/TIS11D gene was detected in a patient with acute myeloid leukemia.[47] Moreover, overexpression of wild-type of *ZFP36L2/TIS11D* gene inhibited growth of HeLa cells.[47] In colorectal cancer, expression of ZFP36 was significantly reduced in cancer tissues and restored ZFP36 expression inhibited epithelial-to-mesenchymal transition and induces a higher susceptibility to anoikis.[48] These studies indicate that *ZFP36L2* acts as a tumor suppressor in human cancers.

In contrast to previous studies, we showed that overexpression of ZFP36L2 was detected in PDAC clinical specimens and knockdown of *ZFP36L2* significantly inhibited cancer cell aggressiveness in PDAC cell lines. Furthermore, high expression of ZFP36L2 is significantly associated with lymph node metastasis and poor prognosis of patients with PDAC. Our data demonstrated that *ZFP36L2* functions as an

oncogene in PDAC cells and is deeply involved in PDAC pathogenesis.

To investigate the oncogenic function of *ZFP36L2* in PDAC cells, we identified *ZFP36L2*-regulated PDAC pathways using genome-wide gene expression analysis of *si-ZFP36L2*-transfected cells. Downstream genes modulated by *ZFP36L2* were categorized by KEGG pathways. Our data showed that "cell cycle" and "pathways in cancer" pathways were downregulated by *ZFP36L2*. Recent study showed that *ZFP36L1* and *ZFP36L2* were critical roles for developing B lymphocytes regulating cell cycle pathways.[49] The genes involved in these pathways were critical regulators of cancer cell aggressiveness. Current studies indicated that several cell cycle kinases, such as *BUB1* and *PLK1*, were multi-functional genes and contributed to cancer cell migration, invasion and metastasis.[50,51] Moreover, overexpression of *EGFR*, *LAMC2*, *ITGA6* and *ITGA3* was observed in several cancers, including PDAC, and these genes were involved in enhancing EMT and cancer cell migration and invasion.[52–54] Furthermore, *SLC2A1* is also known as *GLUT-1* and regulates the entry of glucose into cells.[55] High expression of SLC2A1 is associated with higher histological grade and larger tumor size.[56] Overexpression of *SLC2A1* increases *MMP-2* expression and enhances cancer cell invasion.[57] These studies have supported our present data of knockdown of *ZFP36L2* in PDAC cells.

The primary finding of the present study is the overexpression of *ZFP36L2* and several *ZFP36L2*-regulated genes that are involved in the pathogenesis of PDAC. A TCGA-based large cohort study and gene expression data indicated that high expression of 10 genes (*CDC45*, *CDK6*, *CCNB2*, *CDK1*, *BUB1*, *CCNB1*, *SLC2A1*, *ITGA3*, *STAT1* and *FAS*) predicted poorer survival of PDAC patients. These findings showed that *ZFP36L2*-mediated pathways are deeply involved in PDAC pathogenesis. The identification of the downstream genes regulated by the *miR-375/ZFP36L2* axis may lead to a better understanding of PDAC aggressiveness.

In conclusion, downregulation of *miR-375* was validated in PDAC clinical specimens, and *miR-375* was shown to function as an antitumor miRNA in PDAC cells. To the best of our knowledge, this is the first report demonstrating that *ZFP36L2* is directly regulated by antitumor *miR-375* and acts to regulate several oncogenic genes. Expression of *ZFP36L2* might be a useful prognostic marker for survival of PDAC patients. The identification of novel molecular pathways and targets regulated by the *miR-375/ZFP36L2* axis may lead to a better understanding of PDAC progression and aggressiveness.

Disclosure Statement

The authors have no conflict of interest to declare.

References

1 Kamisawa T, Wood LD, Itoi T, Takaori K. Pancreatic cancer. *Lancet* 2016; **388**: 73–85.
2 Xu Z, Pothula SP, Wilson JS, Apte MV. Pancreatic cancer and its stroma: a conspiracy theory. *World J Gastroenterol* 2014; **20**: 11216–29.
3 Chrystoja CC, Diamandis EP, Brand R, Ruckert F, Haun R, Molina R. Pancreatic cancer. *Clin Chem* 2013; **59**: 41–6.
4 Corbo V, Tortora G, Scarpa A. Molecular pathology of pancreatic cancer: from bench-to-bedside translation. *Curr Drug Targets* 2012; **13**: 744–52.
5 Das S, Batra SK. Pancreatic cancer metastasis: are we being pre-EMTed? *Curr Pharm Des* 2015; **21**: 1249–55.
6 Zhang Y, Wang Z, Gemeinhart RA. Progress in microRNA delivery. *J Control Release* 2013; **172**: 962–74.
7 Salmanidis M, Pillman K, Goodall G, Bracken C. Direct transcriptional regulation by nuclear microRNAs. *Int J Biochem Cell Biol* 2014; **54**: 304–11.
8 Bartel DP. MicroRNAs: target recognition and regulatory functions. *Cell* 2009; **136**: 215–33.
9 Hou BH, Jian ZX, Cui P, Li SJ, Tian RQ, Ou JR. miR-216a may inhibit pancreatic tumor growth by targeting JAK2. *FEBS Lett* 2015; **589**: 2224–32.
10 Zhang J, Zhao CY, Zhang SH *et al.* Upregulation of miR-194 ontributes to tumor growth and progression in pancreatic ductal adenocarcinoma. *Oncol Rep* 2014; **31**: 1157–64.
11 Yoshino H, Chiyomaru T, Enokida H *et al.* The tumour-suppressive function of miR-1 and miR-133a targeting TAGLN2 in bladder cancer. *Br J Cancer* 2011; **104**: 808–18.
12 Itesako T, Seki N, Yoshino H *et al.* The microRNA expression signature of bladder cancer by deep sequencing: the functional significance of the miR-195/497 cluster. *PLoS ONE* 2014; **9**: e84311.
13 Fukumoto I, Kinoshita T, Hanazawa T *et al.* Identification of tumour suppressive microRNA-451a in hypopharyngeal squamous cell carcinoma based on microRNA expression signature. *Br J Cancer* 2014; **111**: 386–94.
14 Yonemori K, Kurahara H, Maemura K, Natsugoe S. MicroRNA in pancreatic cancer. *J Hum Genet* 2016; doi: 10.1038/jhg.2016.59.
15 Zhang H, Liu T, Yi S, Gu L, Zhou M. Targeting MYCN IRES in MYCN-amplified neuroblastoma with miR-375 inhibits tumor growth and sensitizes tumor cells to radiation. *Mol Oncol* 2015; **9**: 1301–11.
16 Hong S, Noh H, Teng Y *et al.* SHOX2 is a direct miR-375 target and a novel epithelial-to-mesenchymal transition inducer in breast cancer cells. *Neoplasia* 2014; **16**: 27990 e1–5.
17 Shen ZY, Zhang ZZ, Liu H, Zhao EH, Cao H. miR-375 inhibits the proliferation of gastric cancer cells by repressing ERBB2 expression. *Exp Ther Med* 2014; **7**: 1757–61.
18 Yoda S, Soejima K, Hamamoto J *et al.* Claudin-1 is a novel target of miR-375 in non-small-cell lung cancer. *Lung Cancer* 2014; **85**: 366–72.
19 Zhou J, Song S, He S *et al.* MicroRNA-375 targets PDK1 in pancreatic carcinoma and suppresses cell growth through the Akt signaling pathway. *Int J Mol Med* 2014; **33**: 950–6.
20 Yang D, Yan R, Zhang X *et al.* Deregulation of MicroRNA-375 inhibits cancer proliferation migration and chemosensitivity in pancreatic cancer through the association of HOXB3. *Am J Transl Res* 2016; **8**: 1551–9.
21 Stumpo DJ, Broxmeyer HE, Ward T *et al.* Targeted disruption of Zfp36l2, encoding a CCCH tandem zinc finger RNA-binding protein, results in defective hematopoiesis. *Blood* 2009; **114**: 2401–10.
22 Sanduja S, Blanco FF, Dixon DA. The roles of TTP and BRF proteins in regulated mRNA decay. *Wiley Interdiscip Rev RNA* 2011; **2**: 42–57.
23 Leslie H, Sobin MKG, Wittekind C, eds. *International Union Against Cancer (UICC) TNM Classification of Malignant Tumors*, 7th edn. Oxford, UK: Wiley-Blackwell, 2009.
24 Kinoshita T, Nohata N, Hanazawa T *et al.* Tumour-suppressive microRNA-29s inhibit cancer cell migration and invasion by targeting laminin-integrin signalling in head and neck squamous cell carcinoma. *Br J Cancer* 2013; **109**: 2636–45.
25 Kojima S, Chiyomaru T, Kawakami K *et al.* Tumour suppressors miR-1 and miR-133a target the oncogenic function of purine nucleoside phosphorylase (PNP) in prostate cancer. *Br J Cancer* 2012; **106**: 405–13.
26 Nohata N, Hanazawa T, Kinoshita T *et al.* Tumour-suppressive microRNA-874 contributes to cell proliferation through targeting of histone deacetylase 1 in head and neck squamous cell carcinoma. *Br J Cancer* 2013; **108**: 1648–58.
27 Anaya J. OncoLnc: linking TCGA survival data to mRNAs, miRNAs, and lncRNAs. *PeerJ Comput Sci* 2016; **2**: e67.
28 Neuzillet C, Tijeras-Raballand A, Bourget P *et al.* State of the art and future directions of pancreatic ductal adenocarcinoma therapy. *Pharmacol Ther* 2015; **155**: 80–104.
29 Eser S, Schnieke A, Schneider G, Saur D. Oncogenic KRAS signalling in pancreatic cancer. *Br J Cancer* 2014; **111**: 817–22.
30 Nohata N, Hanazawa T, Enokida H, Seki N. microRNA-1/133a and microRNA-206/133b clusters: dysregulation and functional roles in human cancers. *Oncotarget* 2012; **3**: 9–21.
31 Ling H, Fabbri M, Calin GA. MicroRNAs and other non-coding RNAs as targets for anticancer drug development. *Nat Rev Drug Discov* 2013; **12**: 847–65.
32 Zhao WG, Yu SN, Lu ZH, Ma YH, Gu YM, Chen J. The miR-217 microRNA functions as a potential tumor suppressor in pancreatic ductal adenocarcinoma by targeting KRAS. *Carcinogenesis* 2010; **31**: 1726–33.
33 Burk U, Schubert J, Wellner U *et al.* A reciprocal repression between ZEB1 and members of the miR-200 family promotes EMT and invasion in cancer cells. *EMBO Rep* 2008; **9**: 582–9.
34 Zhan Q, Fang Y, Deng X *et al.* The interplay between miR-148a and DNMT1 might be exploited for pancreatic cancer therapy. *Cancer Invest* 2015; **33**: 267–75.

35 Tiwari N, Gheldof A, Tatari M, Christofori G. EMT as the ultimate survival mechanism of cancer cells. *Semin Cancer Biol* 2012; **22**: 194–207.
36 Lamouille S, Subramanyam D, Blelloch R, Derynck R. Regulation of epithelial–mesenchymal and mesenchymal–epithelial transitions by microRNAs. *Curr Opin Cell Biol* 2013; **25**: 200–7.
37 Isozaki Y, Hoshino I, Nohata N *et al.* Identification of novel molecular targets regulated by tumor suppressive miR-375 induced by histone acetylation in esophageal squamous cell carcinoma. *Int J Oncol* 2012; **41**: 985–94.
38 Kinoshita T, Nohata N, Yoshino H *et al.* Tumor suppressive microRNA-375 regulates lactate dehydrogenase B in maxillary sinus squamous cell carcinoma. *Int J Oncol* 2012; **40**: 185–93.
39 Nohata N, Hanazawa T, Kikkawa N *et al.* Tumor suppressive microRNA-375 regulates oncogene AEG-1/MTDH in head and neck squamous cell carcinoma (HNSCC). *J Hum Genet* 2011; **56**: 595–601.
40 Jia L, Huang Y, Zheng Y *et al.* miR-375 inhibits cell growth and correlates with clinical outcomes in tongue squamous cell carcinoma. *Oncol Rep* 2015; **33**: 2061–71.
41 Shi W, Yang J, Li S *et al.* Potential involvement of miR-375 in the premalignant progression of oral squamous cell carcinoma mediated via transcription factor KLF5. *Oncotarget* 2015; **6**: 40172–85.
42 Wang Z, Hong Z, Gao F, Feng W. Upregulation of microRNA-375 is associated with poor prognosis in pediatric acute myeloid leukemia. *Mol Cell Biochem* 2013; **383**: 59–65.
43 Costa-Pinheiro P, Ramalho-Carvalho J, Vieira FQ *et al.* MicroRNA-375 plays a dual role in prostate carcinogenesis. *Clin Epigenetics* 2015; **7**: 42.
44 Song SD, Zhou J, Zhou J, Zhao H, Cen JN, Li DC. MicroRNA-375 targets the 3-phosphoinositide-dependent protein kinase-1 gene in pancreatic carcinoma. *Oncol Lett* 2013; **6**: 953–9.
45 Baou M, Jewell A, Murphy JJ. TIS11 family proteins and their roles in posttranscriptional gene regulation. *J Biomed Biotechnol* 2009; **2009**: 634520.
46 Hodson DJ, Janas ML, Galloway A *et al.* Deletion of the RNA-binding proteins ZFP36L1 and ZFP36L2 leads to perturbed thymic development and T lymphoblastic leukemia. *Nat Immunol* 2010; **11**: 717–24.
47 Iwanaga E, Nanri T, Mitsuya H, Asou N. Mutation in the RNA binding protein TIS11D/ZFP36L2 is associated with the pathogenesis of acute leukemia. *Int J Oncol* 2011; **38**: 25–31.
48 Montorsi L, Guizzetti F, Alecci C *et al.* Loss of zfp36 expression in colorectal cancer correlates to wnt/ss-catenin activity and enhances epithelial-to-mesenchymal transition through upregulation of zeb1, sox9 and macc1. *Oncotarget* 2016; doi: 10.18632/oncotarget.10828.
49 Galloway A, Saveliev A, Lukasiak S *et al.* RNA-binding proteins ZFP36L1 and ZFP36L2 promote cell quiescence. *Science* 2016; **352**: 453–9.
50 Nyati S, Schinske-Sebolt K, Pitchiaya S *et al.* The kinase activity of the Ser/Thr kinase BUB1 promotes TGF-beta signaling. *Sci Signal* 2015; **8**: ra1
51 Wu J, Ivanov AI, Fisher PB, Fu Z. Polo-like kinase 1 induces epithelial-to-mesenchymal transition and promotes epithelial cell motility by activating CRAF/ERK signaling. *Elife* 2016; **5**: e10734.
52 Yilmaz M, Christofori G. EMT, the cytoskeleton, and cancer cell invasion. *Cancer Metastasis Rev* 2009; **28**: 15–33.
53 Choudhary KS, Rohatgi N, Halldorsson S *et al.* EGFR signal-network reconstruction demonstrates metabolic crosstalk in EMT. *PLoS Comput Biol* 2016; **12**: e1004924.
54 Horejs CM. Basement membrane fragments in the context of the epithelial-to-mesenchymal transition. *Eur J Cell Biol* 2016; **95**: 427–40
55 Macheda ML, Rogers S, Best JD. Molecular and cellular regulation of glucose transporter (GLUT) proteins in cancer. *J Cell Physiol* 2005; **202**: 654–62.
56 Basturk O, Singh R, Kaygusuz E *et al.* GLUT-1 expression in pancreatic neoplasia: implications in pathogenesis, diagnosis, and prognosis. *Pancreas* 2011; **40**: 187–92.
57 Ito H, Duxbury M, Zinner MJ, Ashley SW, Whang EE. Glucose transporter-1 gene expression is associated with pancreatic cancer invasiveness and MMP-2 activity. *Surgery* 2004; **136**: 548–56.

Supporting Information

Additional Supporting Information may be found online in the supporting information tab for this article:

Fig. S1. The association between the expression levels of *miR-375* with clinicopathological parameters.

Fig. S2. Effects of *miR-375* inhibition on pancreatic ductal adenocarcinoma (PDAC) cell lines.

Fig. S3. Regulation of putative target genes by *miR-375* in pancreatic ductal adenocarcinoma (PDAC) cells.

Fig. S4. The association between the expression level of *CCNB1* or *CCNB2* and overall survival.